Parametric Modeling of the Cross-Correlation for Large-Scale-Fading of Propagation Channels

Xuefeng Yin[1], Xu Zhou[1], Zhifeng Zhang[1], Myung-Don Kim[2] and Hyun Kyu Chung[2]
[1] School of Electronics and Information Engineering, Tongji University, Shanghai, China
[2] Electronics and Telecommunications Research Institute, Daejeon, Republic of Korea
Email: {yinxuefeng, 09_zhouxu, zhangzf}@tongji.edu.cn, {mdkim, hkchung}@etri.re.kr

***Abstract*— Accurate models of the cross-correlation of the large-scale-fading in different propagation channels is essential for designing wireless systems using distributed transmission topologies, such as the coordinated multi-point (CoMP) transmission system. In this contribution, a new parameter defined as the normalized power of common paths in two propagation channels is applied to modeling the cross-correlation of the large-scale-fading in different channels. The common paths here are referred to as the paths with identical parameters, i.e. the delays, Doppler frequencies, directions of arrival and directions of departure. Under the uncorrelated scattering (US) assumption, a new geometrical approach is proposed for modeling the large-scale-fading cross-correlation. Experimental investigations show that the proposed modeling method can be used to generate channel cross-correlation coefficients consistent with the experimental results to a certain extent. We postulate that the discrepancies observed between the empirical and theoretical results are caused by the unrealistic US assumption.**

***Index Terms*— Coordinated multi-point transmission, cross-correlation, propagation channel, power spectrum, and cross power spectrum.**

I. Introduction

Standards of 3G and 4G wireless communication systems, such as the Long-Term-Evolution-Advanced (LTE-A) defined in 3GPP documents TR36.814 [1] and TR36.300 [2], and the World Interoperabilty for Microwave Access (WiMAX) systems defined in IEEE802.16, specify that transmission techniques in distributed topologies should be used for coverage extension, interference suppression, QoS improvement and assisting the merging of heterogeneous networks [3], [4]. Typical examples of these techniques are the relay techniques [5], the coordinated multi-point (CoMP) transmission techniques [6] and the coordinated beamforming techniques presented recently in the WINNER+ project [7]. The relay techniques contain both the conventional schemes such as the amplify-and-forward, decode/compress-and-forward relay techniques, and the novel cooperative relay schemes.

This work is a result of the IT R&D program of KCC/KCA of Korea [09911-01104, Wideband Wireless Channel Modeling based on IMT-Advanced], the project of the Science and Technology Commission of Shanghai Municipality [10ZR1432700, Multidimensional power spectrum characterization and modeling for wide-band propagation channels], China Education Ministry "New-teacher" Project [20090072120015, Time-Variant Channel Characterization, Parameter Estimation and Modeling], China fundamental education basic research project [Polarization characterization of wireless propagation channel], and China national science foundation project [60903033, Research on low cost hard-fault tolerant techniques for microprocessor].

Designing and performance optimization of the relay and CoMP-based technologies or systems require realistic channel models. The classical channel models, e.g. the 3GPP spatial channel models (SCM) [8], the WINNER II SCM enhanced models [9], and the most recently proposed IMT-Advanced channel models [10] mainly focus on the individual links, rather than the joint characteristics, such as the cross-correlation of the links when they are co-existing. As far as we are concerned, the models for the cross-correlation of large-scale fading are either unavailable or oversimplified [11]. These models are established regardless of the heterogeneity of the environments, and cannot be used to reproduce the randomness of cross-correlated channels required for system-level simulations. It is necessary to find some new approaches for modeling the cross-correlations among co-existing links more accurately.

In this contribution, we are interested at using geometrical ray/path-based modeling methods to generate random realizations of two channels with certain cross-correlation in large scale. We start with deriving the relationship between the cross-correlation of large-scale fading and the cross-power spectrum of two channels. By applying the uncorrelated scattering (US) assumption, a new parameter is defined which can be combined with the conventional geometrical models to generate correlated channels. Furthermore, the impact of the antenna radiation patterns and that of the bandlimited property of transmitted signals on the cross-correlation is analyzed. The effectiveness of the proposed modeling method is evaluated with experimental data collected using a wideband sounder from real measurements.

The rest of the contribution is organized as follows. Section II provides a theoretical analysis of the channel cross-correlation in ideal cases and realistic cases. In Section III, the proposed geometrical method for modeling correlated links is presented. Section IV depicts the experimental investigation results for the consistency between empirical channel cross-correlation and the results computed using the proposed method. Finally, conclusive remarks are made in Section V.

II. Cross-correlation of large-scale-fading for two channels

We consider the case where a propagation channel between a transmitter (Tx) and a receiver (Rx) consists of a certain number, say L of specular paths dispersive in delay τ,

978-1-4673-0990-5/12/$31.00 ©2012 IEEE

Doppler frequency ν, direction of departure (DoD) $\mathbf{\Omega}_1$ and direction of arrival (DoA) $\mathbf{\Omega}_2$. Here $\mathbf{\Omega}_1, \mathbf{\Omega}_2 \in \mathcal{R}^3$ are the unit vectors representing the directions of an electromagnetic wave impinging at the small regions surrounding the Tx and the Rx respectively. For notational convenience, we use $\boldsymbol{\theta} = (\tau, \nu, \mathbf{\Omega}_1, \mathbf{\Omega}_2)$ to represent the dispersion dimensions and $\boldsymbol{\theta}_\ell = (\tau_\ell, \nu_\ell, \mathbf{\Omega}_{1,\ell}, \mathbf{\Omega}_{2,\ell})$ to denote the parameters of the ℓth path. Following the nomenclature in [12], the channel bidirection-delay-Doppler frequency spread function $h(\boldsymbol{\theta})$ can be written as

$$h(\boldsymbol{\theta}) = \sum_{l=1}^{L} \alpha_\ell \delta(\boldsymbol{\theta} - \boldsymbol{\theta}_\ell) \tag{1}$$

with $\delta(\boldsymbol{\theta}-\boldsymbol{\theta}_\ell) = \delta(\tau-\tau_\ell)\delta(\nu-\nu_\ell)\delta(\mathbf{\Omega}_1-\mathbf{\Omega}_{1,\ell})\delta(\mathbf{\Omega}_2-\mathbf{\Omega}_{2,\ell})$. and $\delta(\cdot)$ represents the Dirac delta function.

We use $h_i(\boldsymbol{\theta}), i = 1, 2$ to denote the spread function of the first and the second channel, respectively. Furthermore we assume that for any of the two considered two channels, the spread function $h_i(\boldsymbol{\theta})$ contains two parts: the common part $h_c(\boldsymbol{\theta})$ existing in both channels, and the part $h_{s,i}(\boldsymbol{\theta})$ existing only in the ith channel, i.e.

$$h_i(\boldsymbol{\theta}) = h_c(\boldsymbol{\theta}) + h_{s,i}(\boldsymbol{\theta}). \tag{2}$$

The impulse response (IR) of the ith channel observed at the time instance t, frequency f when the Tx and Rx antennas are located at respectively, $\boldsymbol{r}_1$ and $\boldsymbol{r}_2$, can be written as

$$r_i(\boldsymbol{\zeta}) = \int_{\mathcal{D}} h_i(\boldsymbol{\theta}) \exp\{j2\pi <\boldsymbol{\zeta}\cdot\boldsymbol{\theta}>\} \mathrm{d}\boldsymbol{\theta}, \tag{3}$$

where the Tx and Rx antenna radiation patterns are assumed to be isotropic, $\mathcal{D}$ represents the integral region in multi-dimensional dispersion space, $\boldsymbol{\zeta} = (t, f, \boldsymbol{r}_1, \boldsymbol{r}_2)$ is in the Fourier domain of $\boldsymbol{\theta}$, and $<\cdot>$ represents the inner product of the vectors given as arguments, i.e.

$$<\boldsymbol{\zeta}\cdot\boldsymbol{\theta}>= \nu t + f\tau + <\boldsymbol{r}_1\cdot\mathbf{\Omega}_1/\lambda> + <\boldsymbol{r}_2\cdot\mathbf{\Omega}_2/\lambda> \tag{4}$$

with λ being the wavelength.

We now compute the cross-correlation $C_{12}(\boldsymbol{\zeta})$ of the channel IRs $r_1(\boldsymbol{\zeta})$ and $r_2(\boldsymbol{\zeta})$ observed at the same $\boldsymbol{\zeta}$. Notice that using the same $\boldsymbol{\zeta}$ does not necessarily mean that the considered two channels have the same locations for the transmitters, and for the receivers. The common $\boldsymbol{r}_1$ for both channels indicates that the two transmitters are located at the same position with respect to the center of the region surrounding the Tx respectively. Similar for the receivers. The cross-correlation of the fading coefficients of two channels is a narrow-band parameter. It describes the correlation of the fading observed in large scale. As will be shown later, this large-scale fading correlation actually relies on the correlation of the components in the impulse responses of two channels.

The cross-correlation of the fading coefficients $r_i(\boldsymbol{\zeta}), i = 1, 2$ in large scale can be calculated as

$$\begin{aligned} C_{12}(\boldsymbol{\zeta}) &= \mathrm{E}[r_1(\boldsymbol{\zeta}) r_2(\boldsymbol{\zeta})^*] \\ &= \int_{\mathcal{D}'}\int_{\mathcal{D}} \mathrm{E}[h_1(\boldsymbol{\theta}) h_2^*(\boldsymbol{\theta}')] \\ &\qquad \exp\{j2\pi <\boldsymbol{\zeta}\cdot(\boldsymbol{\theta}-\boldsymbol{\theta}')>\} \mathrm{d}\boldsymbol{\theta}\mathrm{d}\boldsymbol{\theta}'. \end{aligned} \tag{5}$$

where $(\cdot)^*$ denotes the complex conjugate. In (5), $\mathrm{E}[h_1(\boldsymbol{\theta})h_2^*(\boldsymbol{\theta}')]$ is defined to be the cross-power-spectrum $p_{12}(\boldsymbol{\theta}, \boldsymbol{\theta}')$ of the two channels. Applying the uncorrelated scattering (US) assumption, it can be shown that

$$p_{12}(\boldsymbol{\theta}, \boldsymbol{\theta}') = p_c(\boldsymbol{\theta}), \tag{6}$$

where $p_c(\boldsymbol{\theta}) = \mathrm{E}[h_c(\boldsymbol{\theta})h_c^*(\boldsymbol{\theta})]$ is the power spectrum of the common components. Inserting (6) back to (5) yields for the channel cross-correlation $C_{12}(\boldsymbol{\zeta})$

$$\begin{aligned} C_{12}(\boldsymbol{\zeta}) &= \int_{\mathcal{D}} p_c(\boldsymbol{\theta}) \mathrm{d}\boldsymbol{\theta} \\ &= P_c, \end{aligned} \tag{7}$$

where P_c is the average power of the common part in the two channels. We can further compute the channel cross-correlation coefficient $c_{12}(\boldsymbol{\zeta})$ as

$$c_{12}(\boldsymbol{\zeta}) = \frac{C_{12}(\boldsymbol{\zeta})}{\sqrt{P_1 P_2}}, \tag{8}$$

where

$$P_i = \int_{\mathcal{D}} p_i(\boldsymbol{\theta}) \mathrm{d}\boldsymbol{\theta},\ i = 1, 2 \tag{9}$$

with $p_i(\boldsymbol{\theta})$ being the power spectrum of the ith channel, represent the total power of the ith channel. .

We define a parameter, η_i to be the ratio of the power of common components and the total power for the ith channel, i.e.

$$\eta_i = P_c/P_i. \tag{10}$$

Inserting (10) into (8) yields for $c_{12}(\boldsymbol{\zeta})$

$$c_{12}(\boldsymbol{\zeta}) = \sqrt{\eta_1 \eta_2}. \tag{11}$$

It can be shown that $P_i \geq P_c$ is always valid. Thus, $\eta_i, c_{12}(\boldsymbol{\zeta}) \in [0, 1]$ holds.

It is worth mentioning that the expression of the channel IR in (3) is only valid for the case where the communication system has unlimited bandwidth and the antennas are isotropic. However, this is usually not the case in reality. In the case where a bandlimited system with arbitrary antenna radiation patterns is considered, the narrowband IR of a channel observed at $\tilde{\boldsymbol{\zeta}} = (t, \boldsymbol{r}_1, \boldsymbol{r}_2)$ reads

$$r(\tilde{\boldsymbol{\zeta}}) = \int_{\mathcal{D}} h(\boldsymbol{\theta}) R(t-\tau) \exp\{j2\pi\nu t\} c_{\mathrm{Tx}}(\mathbf{\Omega}_1) c_{\mathrm{Rx}}(\mathbf{\Omega}_2) \mathrm{d}\boldsymbol{\theta},$$

where $R(t)$ is the autocorrelation function of the transmitted bandlimited signal, $c_{\mathrm{Tx}}(\mathbf{\Omega})$ and $c_{\mathrm{Rx}}(\mathbf{\Omega})$ denote the response of the Tx and the Rx when they are located at $\boldsymbol{r}_1$ and $\boldsymbol{r}_2$ respectively. The cross-correlation of the fadings of the channels can then be written as:

$$\begin{aligned} C_{12}(\bar{\boldsymbol{\zeta}}) = \int_{\mathcal{D}}\int_{\mathcal{D}} & p_{12}(\boldsymbol{\theta}, \boldsymbol{\theta}') \Lambda(\tau' - \tau) \exp\{j2\pi(\nu - \nu')t\} \\ & c_{1,\mathrm{Tx}}(\mathbf{\Omega}_1) c_{1,\mathrm{Rx}}(\mathbf{\Omega}_2) c_{2,\mathrm{Tx}}^*(\mathbf{\Omega}_1') c_{2,\mathrm{Rx}}^*(\mathbf{\Omega}_2') \mathrm{d}\boldsymbol{\theta}\mathrm{d}\boldsymbol{\theta}' \end{aligned} \tag{12}$$

where $\Lambda(\tau' - \tau) = R(t-\tau)R^*(t-\tau')$ have non-zero values when τ is within a certain range that depends on the bandwidth of the transmitted signal.

It is obvious from (12) that the cross-correlation $C_{12}(\bar{\zeta})$ of the large-scale-fading in channel 1 and channel 2 relies on three items, i.e. the cross-power-spectrum of the two channels, the antenna responses and the bandwidth of the transmitted signals. This implies that when the antenna radiation patterns are changed, e.g. by adjusting the antenna orientation, the cross-correlation of two channels can be adapted. Furthermore, the non-zero span of $\Lambda(\tau)$ can also influence the cross-correlation in the sense that the propagation paths with their delay difference less than the non-zero width of $\Lambda(\tau)$ are actually correlated for the bandlimited system.

III. Parametric Modeling of the Cross-Correlation of the Channels

As described in Section II, the cross-correlation of the channel relies on the propagation, the antenna responses and the system responses. The radiation pattern of underlying antennas and the system response are deterministic and can be determined when a specific communication system is considered. Generating multiple realizations of two cross-correlated channels by using a geometrical stochastic channel model requires the exact value of η_i, $i = 1, 2$. Once η_i, $i = 1, 2$ are specified, path assignment can be performed for both channels. In this section we propose a modeling approach which uses η as a parameter to define the common and non-common propagation paths in two channels.

From (11) we see that under the US assumption, the cross-correlation of the large-scale fading in two channels can be calculated by using η_i for two channels. This inspires the following idea of modeling the cross-correlation by correctly setting multiple paths in such a way that the desired values of η_i are adopted. As an example, we now consider generating multiple propagation channels for a CoMP scenario to illustrate how the proposed method is used to create cross-correlated channels. In this example, the method is implemented in four steps.

Step-1: Follow the stochastic channel models, such as the TR25.996 SCM model [8], the WINNER II SCME [9], and the IMT-Advanced channel models [10], to generate a certain number of clusters of paths for individual channels.

Step-2: Specify the narrowband cross-correlation matrix $\boldsymbol{C}$ of the channels in the CoMP scenario considered. The entries in $\boldsymbol{C}$ can be either obtained from measurements or randomly generated based on a predefined stochastic model.

Step-3: For any pair of the channels, say the ith and the i'th channels, we decompose the cross-correlation coefficients $c_{ii'}$, which is given in ***Step-2***, into $c_{ii'} = \sqrt{\eta_i \eta_{i'}}$. One simply way for performing the decomposition is to make $\eta_i = \eta_{i'} = \sqrt{c_{ii'}}$.

Step-4: For simplicity, we assume that for any pair of channels, there is always one common cluster existing in both channels. The parameter η_i specifies the ratio of the power of common clusters to the total power of the clusters. Therefore, the common cluster's power P_c can be set to be $P_c = \eta_i P_i$. The other settings of the paths, such as the initial phases, azimuths, delays and Doppler frequencies can follow the rules defined in the standard models.

(a) Office scenario (b) Corridor scenario

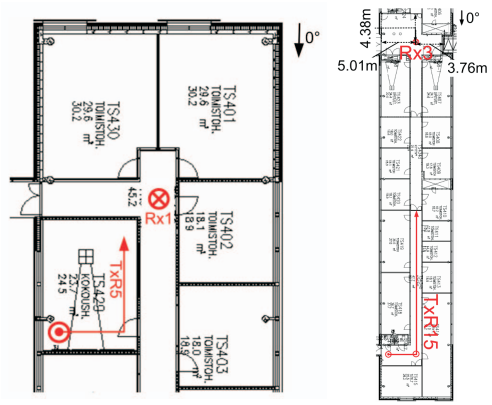

Fig. 1. The maps of the environment and the routes for measurements in the office scenario (a) and the corridor scenario (b).

IV. Experimental Evaluation of the Parametric Modeling of the Cross-Correlation

In this section, we use measurement data to evaluate the effectiveness of using the parameter η to model the cross-correlation of channels. The evaluation is conducted in the following procedure:

1) The cross-correlation coefficients c_{ij} of the large-scale-fading of the channels i and j are calculated using the measurement data.
2) The parameter estimation algorithm – Space-Alternating Generalized Expecation-maximization (SAGE) [13] – is used to estimate multiple paths from individual channels.
3) Based on the SAGE estimation results, the parameters η_i and η_j are calculated for the ith and jth channels.
4) The cross-correlation coefficient $\hat{c}_{ij}$ is calculated with $\hat{c}_{ij} = \sqrt{\eta_i \eta_j}$, and compared with c_{ij} obtained in 1).

The measurements were organized by Technology University of Vienna and Elektrobit in Oulu University, using the wideband MIMO channel sounder - Propsound [14]. For the detail description of the sounder and the measurement campaign, readers are referred to [15]. The Tx and Rx were equipped with antenna array of 50 and 32 elements respectively. The Rx was fixed in the measurements. The Tx was moving along specific routes at speed about 0.5 m/s. The bandwidth of the sounder equals 100 MHz. The carrier frequency was 5.25 GHz. Channels between all Tx antennas and Rx antennas are measured sequentially in time-division-multiplexing (TDM) mode. In each measurement cycle, $50 \times 32 = 1600$ subchannels are measured once. The data is acquired during a burst which consists of the four consecutive cycles. Then after waiting for the duration of 12 cycles, the data acquisition is activated again. The movement of the Tx in cycle is negligible, so that the channel can be assumed invariant within the period of one cycle. The radiation patterns are not the same for

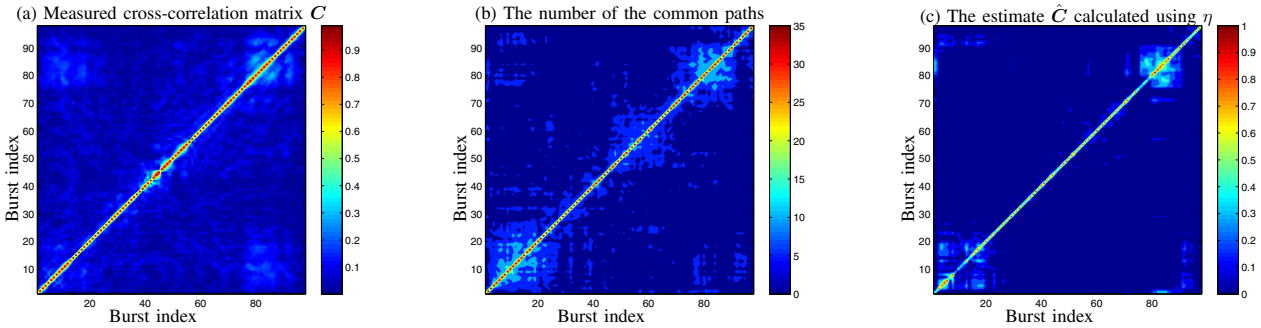

Fig. 2. The cross-correlation coefficients of channels measured in the office scenario (a), the number of paths that are considered to be common in both channels (b) and the cross-correlation coefficients calculated by using the parameter η (c).

the Tx and Rx antennas. In addition, the system responses suffer from random phase noise when measuring different subchannels. Thus, it is reasonable to consider that the channel impulse responses obtained from the 1600 subchannels are independent observations of the wide-sense-stationary channel. The narrowband channel coefficients are calculated by summing up the impulse responses of individual subchannels. The cross-correlation coefficient c_{ij} of the channel i and j is then calculated as

$$c_{ij} = |\mathrm{E}[r_i {r_j}^*] - \mu_i \mu_j| / (\sigma_i \sigma_j), \tag{13}$$

where $\mu_{i/j}$ and $\sigma_{i/j}$ denote respectively the mean and standard deviation of the channel i/j.

The measurement data obtained in two indoor scenarios, i.e. an office and a corridor, are used for evaluating the proposed modeling method for the large-scale-fading cross-correlation among channels. The maps of the environments for both scenarios are shown in Fig. 1. In the office scenario, the measurement was performed with the Tx moving in an office from the locations marked with a solid red spot, and stopped at the location marked with an arrow, and the Rx was fixed in the turn of a corridor. In the corridor scenario, the Tx moved along a route through a corridor with office rooms along the corridor. It is worth mentioning that the measurements conducted in the corridor can be divided into two parts, the non-line-of-sight (NLOS) and the line-of-sight (LOS) scenarios.

Fig. 2 (a) depicts the absolute value of the cross-correlation coefficients of the fadings on the channels calculated using (13) for the office scenario. The $x-$ and $y-$axes represent the burst indices. Fig. 2 (b) depicts the number of paths that are considered to be common in both channels. The paths in different channels are considered to be the same when the difference of the parameters of the paths is below the intrinsic resolution of the sounding system imposed by the width of the mainlobe of the power spectrum. For example, in the azimuth domain, for the antenna array used, the range is set to 14°. It can be observed from Fig. 2 (b) that the pattern of the path number is similar with that of the cross-correlation coefficients. Fig. 2 (c) depicts the estimate $\hat{c}_{12}$ of the cross-coefficients computed using (11) with η_1 and η_2 estimated from the SAGE estimation results. It can be seen that Fig. 2 (a) and (c) look similar. However, the differences between Fig. 2 (a) and (c) are also observed.

Fig. 3 (a), (b) and (c) depict for the corridor scenario, the measured channel cross-correlation matrix $\boldsymbol{C}$, the number of common paths in all possible pairs of channels, and the estimate $\hat{\boldsymbol{C}}$ of the cross-correlation matrix computed using (11) with the parameters η_1 and η_2 calculated from the SAGE estimation results respectively. It can be observed that some portions of $\hat{\boldsymbol{C}}$ shown in Fig. 3 (c) are similar with their counterparts in $\boldsymbol{C}$ as shown in Fig. 3 (a). However, we also observe the non-consistency between $\boldsymbol{C}$ and $\hat{\boldsymbol{C}}$, e.g. the exact values of $\hat{c}_{12}$ are different from the measured c_{12}. For some points where c_{12} is non-zero, the estimates $\hat{c}_{12}$ are equal to zeros.

We postulate that the discrepancy between $\boldsymbol{C}$ and $\hat{\boldsymbol{C}}$ as observed in Fig. 2 and Fig. 3 are caused by the following reasons:

1) The estimates $\hat{c}_{12}$ of the cross-correlation coefficients are computed by assuming isotropic antenna responses. This implies that the influence of the non-isotropic antennas used in the measurements on channel cross-correlation is not considered. However, the measured c_{12} is obtained by taking into account the realistic antenna radiation pattern and the property of the sounding signal. This difference may result in errors for the estimate $\hat{c}_{12}$.
2) The parameters η_1 and η_2 are computed based on the 20 estimated paths. This number can be too low to obtain the accurate estimates of η_1 and η_2.
3) The US assumption may not hold in reality for some of the propagation paths. This may be due to the fact that when paths belonging to a bin with width equal to the non-zero span of $\Lambda(\tau)$, the paths can be correlated even in the case where the angular parameters and Doppler frequency of the paths are different. Further studies are necessary to find appropriate parameters and methods for modeling the large-scale-fading cross-correlation in such cases..

V. Conclusions

In this contribution, we introduced a new parameter η that can be used for modeling the cross-correlation of the large-scale-fading of multiple channels using geometrical approaches.

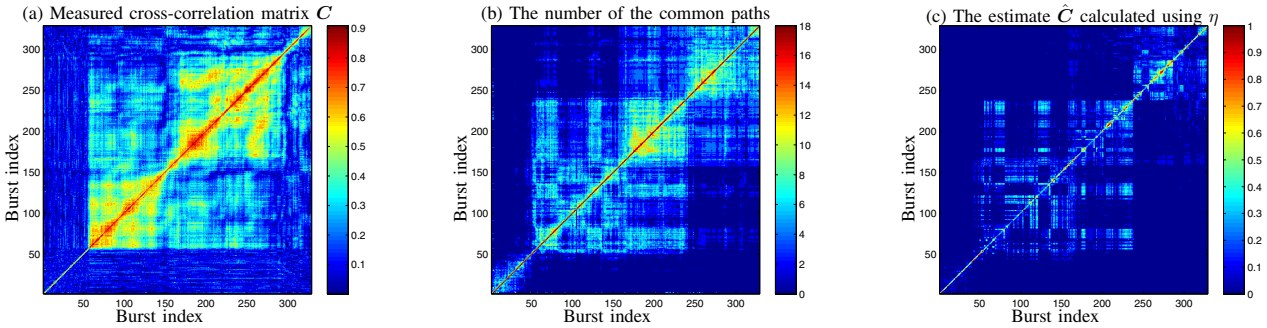

Fig. 3. The cross-correlation coefficients of the channel coefficients observed in the corridor scenario (a), the number of common paths in two channels (b), and c_{12} computed based on η_1 and η_2 using (11) (c).

This parameter is defined to be the ratio of the power of common paths in two channels to the total power of individual channels. The common paths are referred to as the paths existing in different links with similar geometrical parameters, such as delay, Doppler frequency, direction of arrival and direction of departure. Based on the newly-defined parameter, we proposed a new approach for modeling and simulating the multiple propagation channels that are cross-correlated in large scale fading. Measurement results showed that this parametric modeling approach can be used to describe the cross-correlation of channels to some extent. It is our conjecture that the discrepancy between the measured results and the estimates calculated based on the proposed model is due to the facts that the antenna radiation patterns are not taken into account, and that the uncorrelated scattering assumption on which the proposed model relies may be invalid in real measurement environments.

ACKNOWLEDGEMENT

The authors wish to acknowledge Nicolai Czink, from ftw. for kindly providing the measurement data.

REFERENCES

[1] *3GPP TR36.814 V9.0.0 (2009) Further Advancements for Evolved Universal Terrestrial Radio Access (EUTRA) Physical Layer Aspects (Release 9)*, 3rd Generation Partnership Project; Technical Specification Group Radio Access Network Std., 2009.

[2] *3GPP TS 36.300 v8.7.0 Evolved Universal Terrestrial Radio Access (EUTRA) and Evolved Universal Terrestrial Radio Access Network (EUTRAN); Overall description; Stage 2*, 3rd Generation Partnership Project; Technical Specification Group Radio Access Network Std., Dec. 2008.

[3] H. Dai, H. Zhang, and Q. Zhou, "Some analysis in distributed MIMO systems," *Journal of Communications*, vol. 2, no. 3, pp. 43–50, May 2007.

[4] "IEEE 802.16's Relay Task Group: IEEE 802.16j proposals." IEEE, 2009.

[5] Y. Fan and J. Thompson, "MIMO Configurations for Relay Channels: Theory and Practice," *IEEE Transactions on Wireless Communications*, vol. 6, no. 5, pp. 1774 –1786, may. 2007.

[6] M. Karakayali, G. Foschini, and R. Valenzuela, "Network coordination for spectrally efficient communications in cellular systems," *IEEE Transactions on Wireless Communications*, vol. 13, no. 4, pp. 56 –61, aug. 2006.

[7] M. Boldi, C. Botella, F. Boccardi, V. D. Amico, E. Hardouin, M. Olsson, H. Pennanen, P. Rost, V. Savin, T. Svensson, and A. Tolli, "D1.8 Intermediate Report on CoMP," *Wireless World Initiative New Radio (WINNER+)*, p. 75, 2010.

[8] "Spatial channel model for Multiple Input Multiple Output (MIMO) simulations (Release 7)," 3GPP TR25.996 V7.0.0, 2007.

[9] P. Kyosti, J. Meinila, L. Hentila, X. Zhao, T. Jamsa, C. Schneider, M. Narandzic, M. Milojevic, A. Hong, J. Ylitalo, *et al.*, "Winner II channel models," *European Commission, Deliverable IST-WINNER D*, vol. 1.

[10] "Guidelines for evaluation of radio interface technologies for IMT-Advanced," Rep. ITU-R M.2135, 2008.

[11] C.-X. Wang, X. Hong, X. Ge, X. Cheng, G. Zhang, and J. Thompson, "Cooperative mimo channel models: A survey," *Communications Magazine, IEEE*, vol. 48, no. 2, pp. 80 –87, Feb. 2010.

[12] B. H. Fleury, "First- and second-order characterization of direction dispersion and space selectivity in the radio channel," *IEEE Transactions on Information Theory*, vol. 46, no. 6, pp. 2027–2044, september 2000.

[13] X. Yin, B. H. Fleury, P. Jourdan, and A. Stucki, "Polarization estimation of individual propagation paths using the SAGE algorithm," in *Proceedings of the IEEE International Symposium on Personal, Indoor and Mobile Radio Communications (PIMRC)*, Beijing, China, Sept. 2003.

[14] P. Kyösti, J. Meinilä, L. Hentilä, X. Zhao, T. Jämsä, C. Schneider, M. Narandzić, M. Milojević, A. Hong, J. Ylitalo, V.-M. Holappa, M. Alatossava, R. Bultitude, Y. de Jong, and T. Rautiainen, "WINNER II Channel Models D1.1.2 V1.1," no. IST-4-027756 WINNER II, D1.1.2 V1.1, 11 2007.

[15] N. Czink, "The Random-Cluster Model - A Stochastic MIMO Channel Model for Broadband Wireless Communication Systems of the 3rd Generation and Beyond," Ph.D. dissertation, Technology University of Vienna, Department of Electronics and Information Technologies, December 2007.